

Supporting information

Two-Colour Photoswitching in Photoresponsive Inorganic Thin Films

Elin Sundin, Fredrik Johansson, Valeria Saavedra Becerril, Joachim Wallenstein, August Gasslander, Jerker Mårtensson, Maria Abrahamsson*

*Department of Chemistry and Chemical Engineering, Chalmers University of Technology,
Gothenburg, Sweden*

**Corresponding author: abmaria@chalmers.se*

Contents

Synthesis.....	S3
Proton and carbon NMR spectra.....	S5
High-resolution mass spectrum.....	S8
Additional photoisomerization experiments.....	S9
Quantum yield calculations.....	S14
References	S16

Synthesis

Starting materials and solvents were purchased from commercial vendors and used as received. Dry tetrahydrofuran was prepared by distillation over sodium under nitrogen atmosphere. Glassware for reactions was dried in an oven prior to use. Column chromatography was performed on an automated column chromatography Biotage Isolera™ Spektra One using Biotage SNAP® 10 g KP-sil, 25 g KP-sil and 30 g KP-C18-HS columns. Thin layer chromatography (TLC) was carried out on Merck silica gel on aluminum sheets, both 60-F₂₅₄ and 60 RP-18 F₂₅₄S, and analyzed using a mercury vapor UV-lamp (254 nm and 365 nm). The used pressure reactor was a 50 mL Teflon lined Hydrothermal synthesis Autoclave Reactor purchased from Hydriion Scientific and consist of a Teflon container placed in a metal casing with specified allowed range up to 220 °C and 3 MPa. NMR was collected using an Agilent 400 MHz or Bruker 800 MHz spectrometer on samples dissolved in either deuterated chloroform (chloroform-d) or acetonitrile (acetonitrile-d₃). The chemical shifts are reported in parts per million δ (ppm) relative a residual peak; chloroform (¹H: δ = 7.26 ppm, ¹³C: δ = 77.16 ppm), acetonitrile (¹H: δ = 1.94 ppm, ¹³C: δ = 1.32 ppm). Multiplicities are indicated by; s (singlet), d (doublet), dd (doublet of doublet), t (triplet), q (quartet) and m (multiplet). Coupling constants (*J*) are reported in Hz. High-resolution mass determinations were performed on a Xevo G2-XS QTOF instrument, equipped with an electrospray interface operated in positive-ionization mode. The samples were analyzed by flow injection ESI-MS using the following mobile phase composition: 10 % mobile phase A (water plus 0.04% formic acid) and 90% mobile phase B (methanol plus 0.04% formic acid).

2,2'-bipyridine-4,4'-bis(ethoxycarbonyl) (deeb): 2,2'-Bipyridine-4,4'-dicarboxylic acid (200 mg, 0.82 mmol) was brought to reflux in 50 mL ethanol with 0.5 mL conc. H₂SO₄ for 16 h. The solvent was then removed by rotary evaporation. The crude mixture was dissolved in 20 mL water and 2 M NaOH was added until the pH reached 7. The precipitation was filtered off and dried, resulting in the product as a white powder. Yield: 219 mg (89 %). ¹H NMR (CDCl₃, 400 MHz): 8.95 (dd, *J* = 0.9, 1.3, 1H), 8.87 (dd, *J* = 0.7, 5.0, 1H), 7.91 (dd, *J* = 1.6, 5.0, 1H), 4.46 (q, *J* = 7.1, 2H), 1.45 (t, *J* = 7.1, 3H)

2-(propane-2-sulfanylmethyl)-pyridine (PySiPr): 2-(Chloromethyl)pyridine hydrochloride (830 mg, 5.06 mmol) and NaOH (403 mg, 10.1 mmol) were added to 50 mL acetonitrile and heated to 50 °C until all reagents were dissolved. Sodium 2-propanthiolate (580 mg, 5.92 mmol) was then added and the mixture was refluxed for 3 h. The solvent was removed using rotary evaporation before extracteion using 20 mL water and 3 x 20 mL dichloromethane. The combined organic phase was dried over Na₂SO₄, filtered and concentrated *in vacuo*. The product was collected as a red oil. Yield: 662 mg (78 %). ¹H NMR (CDCl₃, 400 MHz): 8.52 (d, 1H), 7.64 (t, 1H), 7.4 (d, 1H), 7.15 (t, 1H), 3.88 (s, 2H), 2.89 (m, 1H), 1.27 (d, 6H)

2-(propane-2-sulfinylmethyl)-pyridine (PySOiPr): PySiPr (400 mg, 2.39 mmol) was dissolved in 30 mL 1:1 mixture of water and methanol. Sodium periodate was dissolved in 10 mL water and this mixture was then added dropwise to the PySiPr solution. The reaction was stirred for 20 min before all solvent was removed using rotary evaporation. The product was collected as a yellow oil. Yield: 350 mg (80 %) ¹HNMR (CDCl₃, 400 MHz): 8.62-8.58 (m, 1H), 7.72-7.67 (m, 1H), 7.44-7.37 (m, 1H), 7.23-7.28 (m, 1H), 4.14 (d, *J* = 12.8, 1H), 4.01 (d, *J* = 12.8, 1H), 2.87-2.79 (m, 1H), 1.36-1.31 (m, 1H)

cis-Ru(deeb)₂Cl₂: RuCl₃•nH₂O (200 mg, 0,89 mmol) and deeb (533 mg, 1.77 mmol) were dissolved in 5 mL DMF and refluxed for 16 h. The solvent was then removed using rotary evaporation and later replaced with 5 mL methanol. The mixture was subsequently put in the refrigerator overnight before the formed precipitate was filtered off, washed using cold methanol and finally air dried. The product was collected as a black powder. Yield: 444 mg (65%). ¹H NMR (CDCl₃, 400 MHz): 10.25 (dd, 5.9, 0.8, 1H), 8.96 (dd, *J* = 1.8, 0.7, 1H), 8.78 (dd, *J* = 1.8, 0.7, 1H), 8.20 (dd, *J* = 5.9, 1.8, 1H), 7.79 (dd, *J* = 6.0, 0.7, 1H), 7.64 (dd, *J* = 6.0, 1.8, 1H), 4.53 (q, *J* = 7.1, 4H), 4.37 (q, *J* = 7.1 4H), 1.49 (t, *J* = 7.1, 6H), 1.36 (t, *J* = 7.1, 6H) ¹³C NMR (101 MHz, CDCl₃) δ 164.13 163.61 160.39 158.02 155.13 152.50 136.35 135.03 124.96 124.48 121.84 121.58 62.61 62.45 14.34 14.22

[Ru(deeb)₂PySOiPr][PF₆]₂: Ru(deeb)Cl₂ (50 mg, 0.065 mmol) and PySOiPr (12 mg, 0.065 mmol) were dissolved in 10 mL ethanol and was refluxed together with 2 equivalents of silver hexafluorophosphate (33 mg, 0.13 mmol)

for 24 h. The reaction mixture was then put in the freezer overnight and the formed precipitate was filtered and washed using small amounts of cold ethanol. The precipitate was thereafter washed with acetonitrile and the collected filtrate from this later wash was concentrated *in vacuo*. The product, obtained as mixture of diastereomers, was collected as a red powder. Yield: 60 mg (77 %) ^1H NMR (CD_3CN , 800 MHz): 10.19 (dd, $J = 5.9$, 0.6, 1H), 9.17-9.14 (m, 2H), 9.12 (dd, $J = 1.8$, 0.6, 1H), 9.04 (dd, $J = 1.8$, 0.6, 1H), 9.03-9.00 (m, 3H), 8.96 (dd, $J = 1.8$, 0.6, 1H), 8.89 (d, $J = 5.9$, 1H), 8.22 (dd, $J = 5.9$, 1.8, 1H), 8.19 (d, $J = 1.2$, 2H), 8.16-8.13 (m, 2H), 8.07-7.88 (m, 6H), 7.86-7.73 (m, 6H), 7.58-7.56 (m, 1H), 7.35-7.26 (m, 3H), 7.21-7.16 (m, 1H), 5.17 (d, $J = 17.4$, 1H), 5.14 (d, $J = 17.0$, 1H), 5.04 (d, $J = 17.4$, 1H), 4.70 (d, $J = 17.0$, 1H), 4.60-4.40 (m, 16H), 4.04-3.97 (m, 1H), 2.35-2.28 (m, 1H), 1.55-1.33 (m, 30H), 0.67 (d, $J = 6.7$, 3H), 0.39 (d, $J = 6.7$, 3H) ^{13}C NMR (201,2 MHz, CD_3CN) δ 164.30 164.21 164.06 164.02 164.01 163.98 163.91 163.79 158.80 158.41 158.25 158.24 158.15 158.02 157.98 157.88 157.68 157.31 157.14 156.68 155.08 154.95 154.84 154.26 153.22 153.22 153.19 151.94 142.25 142.24 142.09 141.79 141.67 141.54 141.53 141.40 140.56 140.55 129.70 128.55 128.48 128.09 127.97 127.77 127.52 127.26 127.16 126.80 126.73 126.29 125.46 125.43 125.41 125.09 124.77 124.67 65.04 64.66 64.03 63.89 63.87 63.85 63.83 63.79 63.74 57.48 56.53 16.26 16.01 15.20 14.71 14.44 14.41 14.38 14.32 14.31. HRMS (ESI-QTOF) m/z : $[\text{M} - \text{PF}_6]^+$ calc for $\text{C}_{41}\text{H}_{45}\text{F}_6\text{N}_5\text{O}_9\text{PRuS}$, 1030,162; found, 1030.165.

Proton- and carbon-NMR spectra

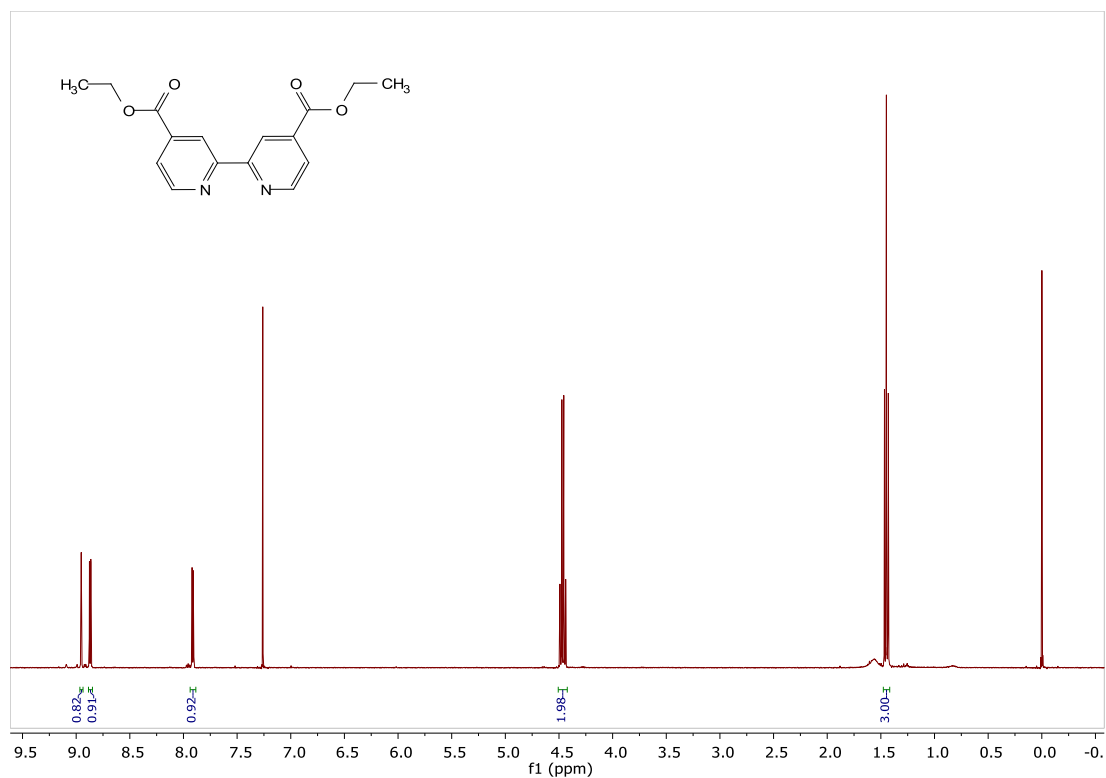


Figure S1. ¹H NMR: 2,2'-bipyridine-4,4'-bis(ethoxycarbonyl) (deeb) in chloroform-d.

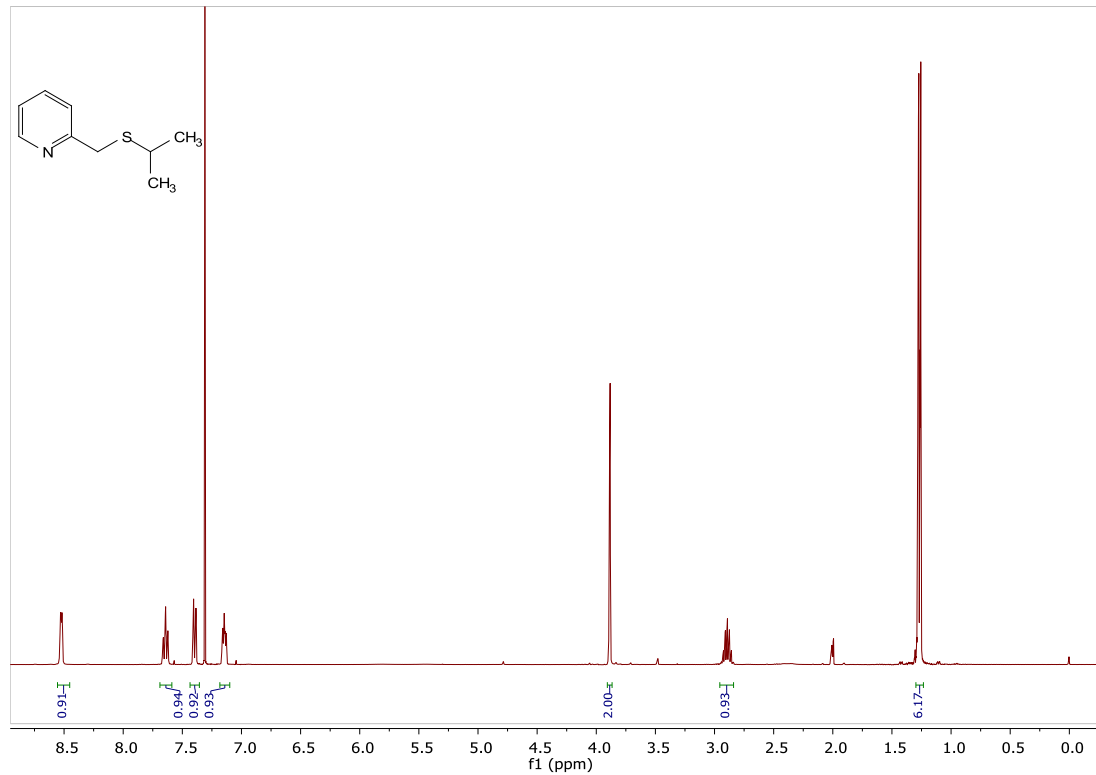


Figure S2. ¹H NMR: 2-(propane-2-sulfanylmethyl)-pyridine (PySiPr) in chloroform-d.

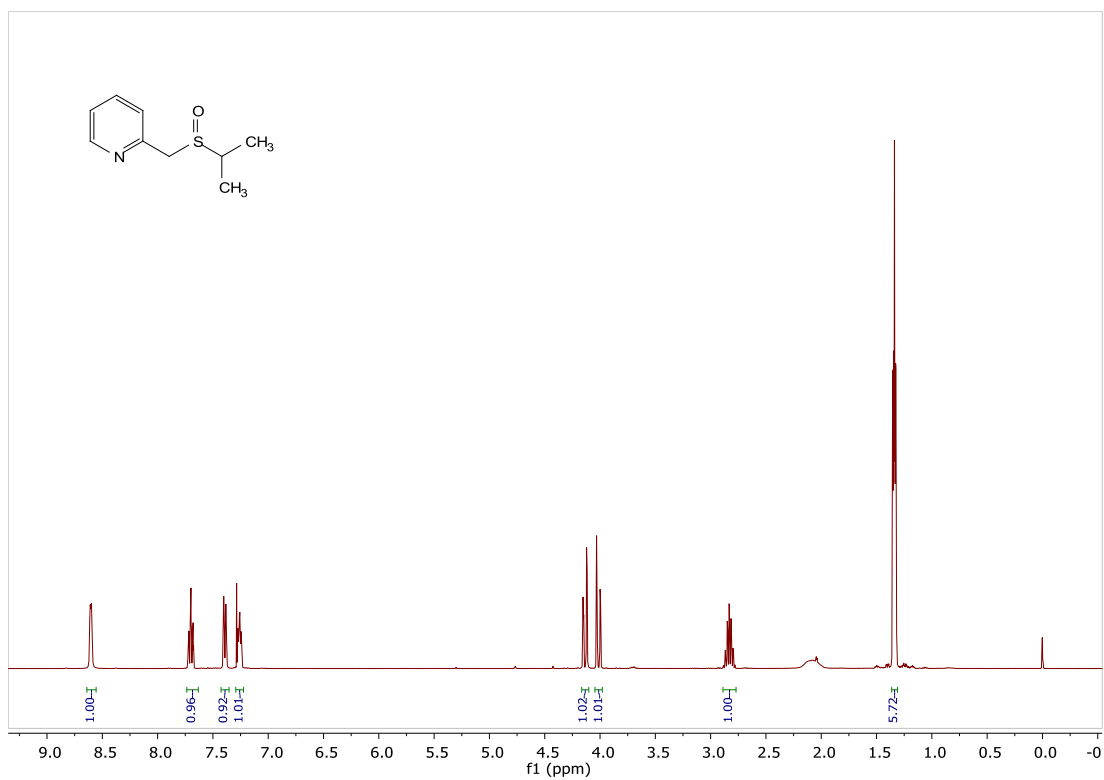


Figure S3. ¹H NMR: 2-(propane-2-sulfinylmethyl)-pyridine (PySOiPr) in chloroform-d.

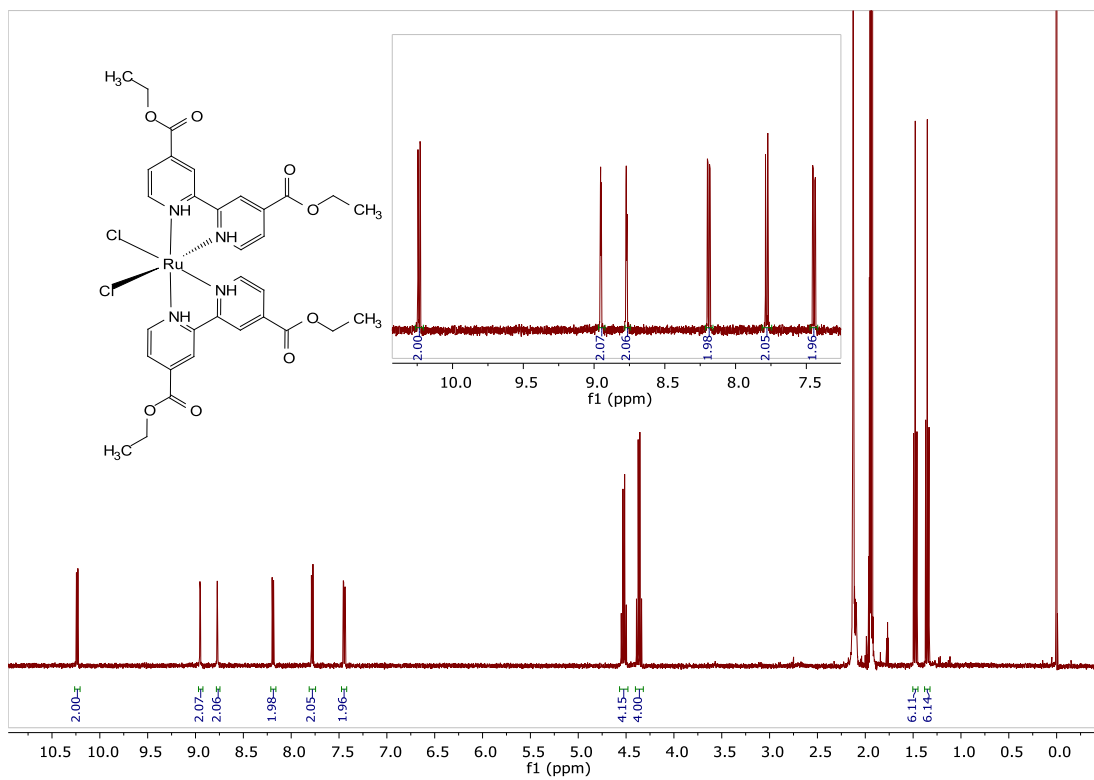


Figure S4. ¹H NMR: Ru(deeb)₂Cl₂ in chloroform-d.

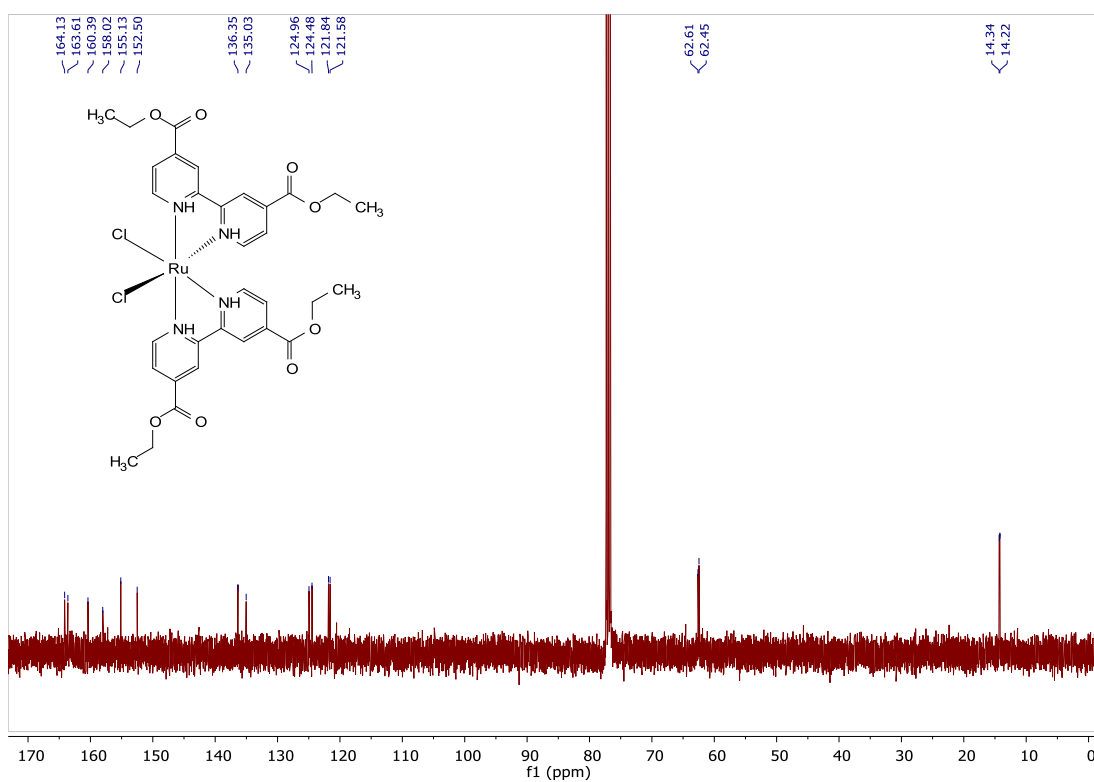


Figure S5. ^{13}C NMR: $Ru(deeb)_2Cl_2$ in chloroform- d .

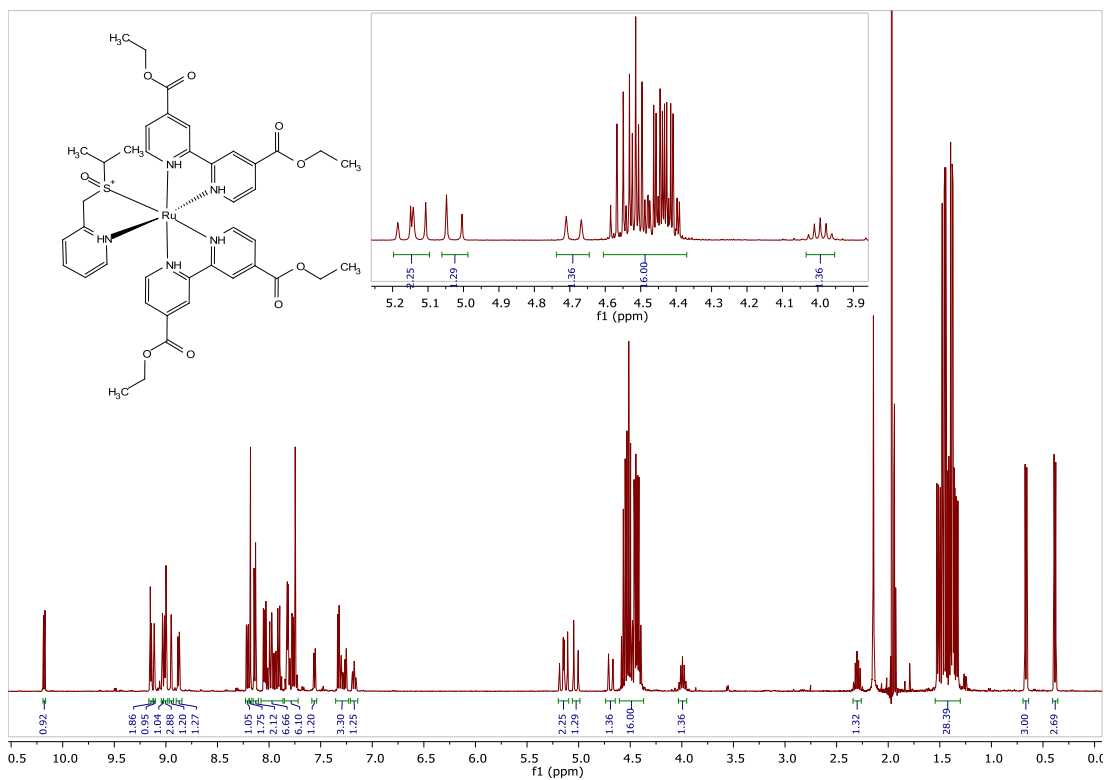


Figure S6. 1H NMR: $[Ru(deeb)_2PySOiPr][PF_6]_2$ in acetonitrile- d_3 .

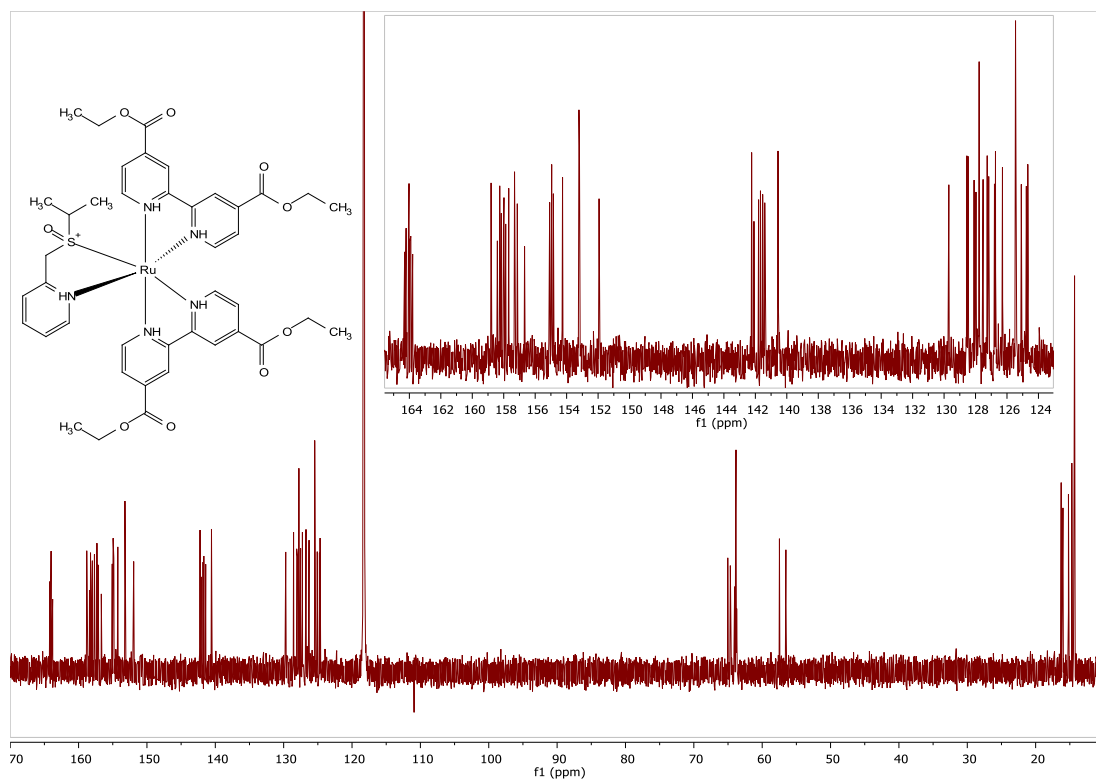
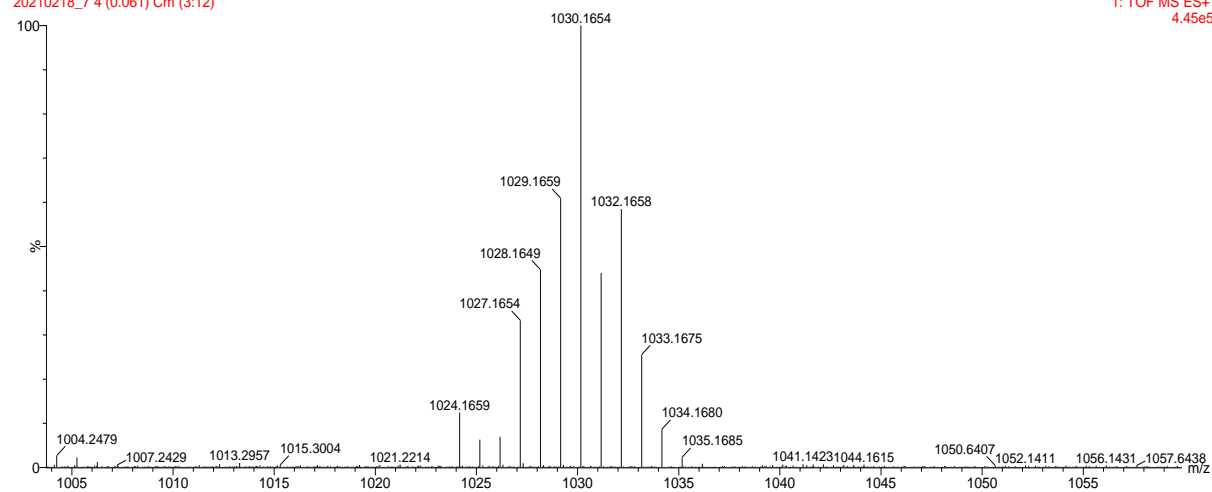


Figure S7. ^{13}C NMR: $[Ru(deeb)_2PySOiPr][PF_6]_2$ in acetonitrile- d_3

High-resolution mass spectrum

WMM 1:10 dil Jerker
20210218_7 4 (0.061) Cm (3:12)



1: TOF MS ES+
4.45e5

Figure S8. Magnified mass spectrum for the $[M - PF_6]^+$ ion of compound $[Ru(deeb)_2PySOiPr][PF_6]_2$.

Additional photoisomerization experiments

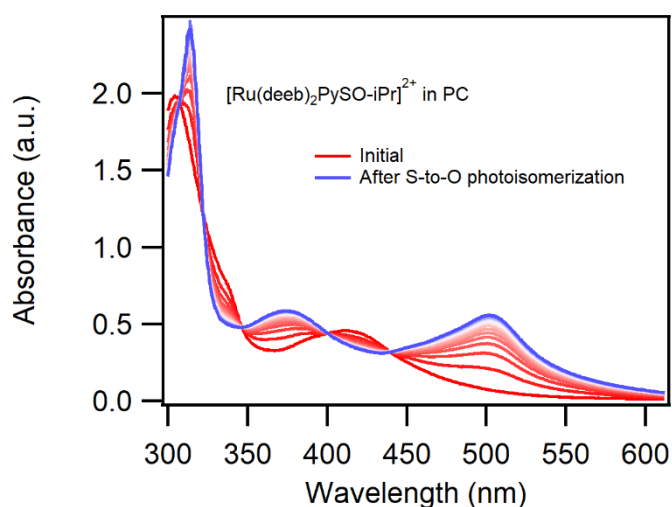


Figure S9. Absorption changes of $[Ru(deeb)_2PySO-iPr]^{2+}$ in PC solution continuously irradiated with 385 nm light (from red to blue spectra, 1 min between each measurement). The absorption changes represent S-to-O photoisomerization of the complex.

Irradiation in MeCN solution leads to an initial S-to-O photoisomerization followed by irreversible absorption changes with a new set of isosbestic points (Figure S9), attributed to ligand exchange of the sulfoxide ligand with the solvent^{S1} in agreement with the irreversibility and with previous studies in donor solvents^{S2}.

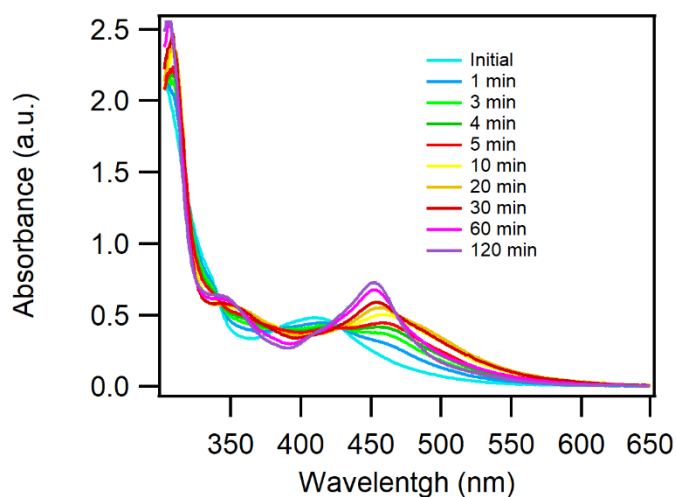


Figure S10. Absorption changes of $[Ru(deeb)_2PySO-iPr]^{2+}$ in MeCN solution continuously irradiated with 385 nm light. The absorption changes represent S-to-O photoisomerization of the complex followed by ligand exchange with the solvent.

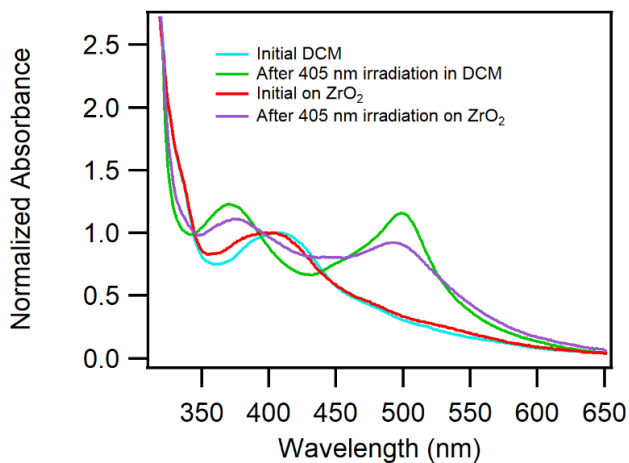


Figure S11. Normalized absorption spectra before and after irradiation with 405 nm light until no further spectra changes are observed of $[Ru(deeb)_2PySO-iPr]^{2+}$ in DCM solution and attached to a ZrO_2 thin film.

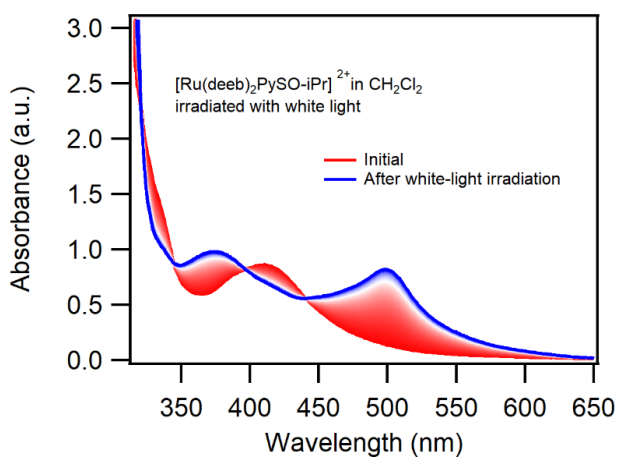


Figure S12. Absorption changes of $[Ru(deeb)_2PySO-iPr]^{2+}$ in DCM solution continuously irradiated with white-light. The absorption changes represent S-to-O photoisomerization of the complex.

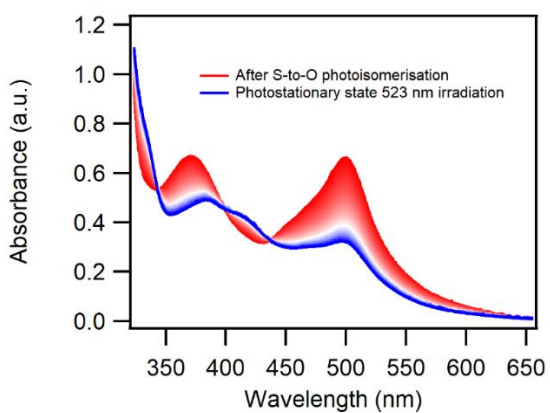


Figure S13. Absorption changes of $[Ru(deeb)_2PySO-iPr]^{2+}$ in DCM solution continuously irradiated with 523 nm light.

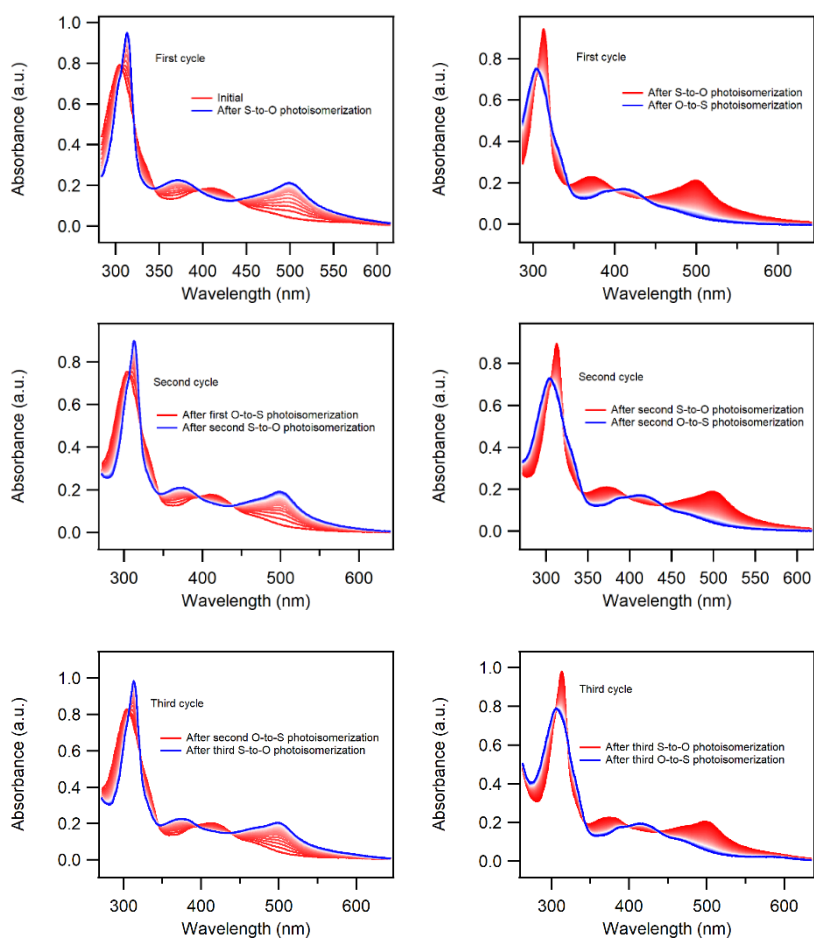


Figure S14. Absorption changes following repeated photoisomerization in DCM solution with 385 nm light for the S-to-O photoisomerization (30 s between each scan, $t_{final} \sim 15$ min) and 623 nm light for the O-to-S photoisomerization (5 min between each scan, $t_{final} \sim 10$ hours).

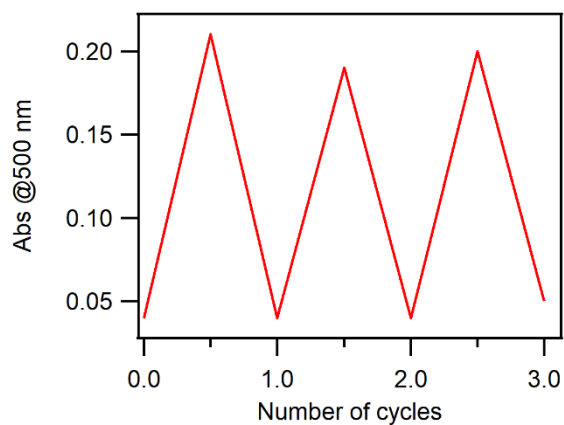


Figure S15. Absorption at 500 nm after each cycle of the S-to-O and O-to-S photoisomerization of the complex in DCM liquid solution.

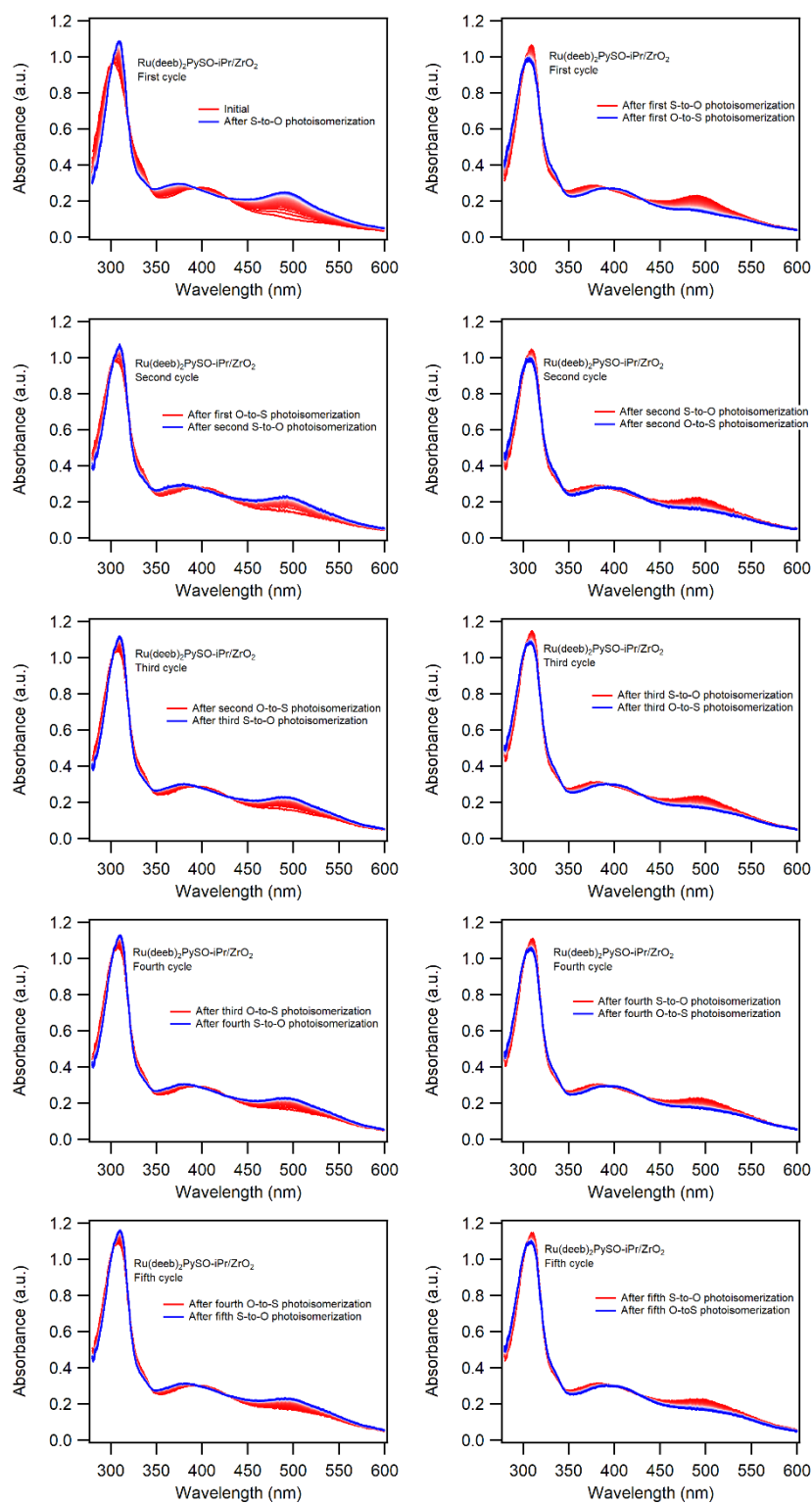


Figure S16. Absorption changes following repeated photoisomerization of the complex attached to ZrO_2 with 405 nm light for the S-to-O photoisomerization (30 s between each scan, $t_{final} \sim 30$ min) and 623 nm light for the O-to-S photoisomerization (5 min between each scan, $t_{final} \sim 20$ hours).

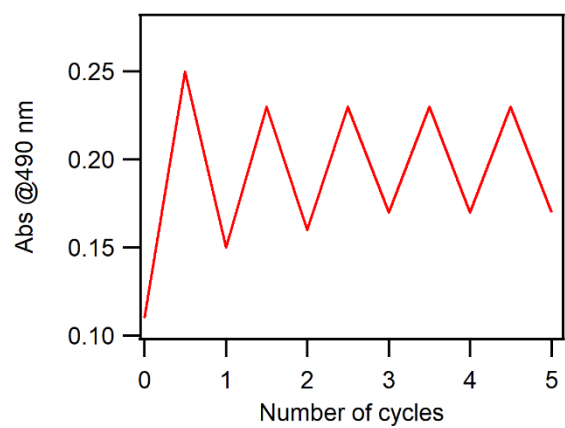


Figure S17. Absorption at 490 nm after each cycle of the S-to-O and O-to-S photoisomerization of the complex attached to ZrO_2 .

S-to-O quantum yield of photoisomerization

The S-to-O photoisomerization quantum yield was estimated using ferrioxalate actinometry in a similar way as previously reported methods⁵³⁻⁵. To calculate the light intensity (I), a known volume (v_1) of a solution of 0.006-0.15 M ferrioxalate (0.006 M for 365 nm irradiation and 0.03-0.15 for 405 nm irradiation) was irradiated for a time t , and an aliquot of the irradiated solution (v_2) was mixed with a phenanthroline solution, diluted (v_3) and left to react for at least 30 min. The absorption at 510 nm was then measured. This was repeated using different times ($t=0$ to $t=2$ min) and the slope of the absorption at 510 nm vs time was then used to calculate I with equation 1

$$I = \text{slope} * \frac{v_1 * v_3}{v_2 * \epsilon_{510} * l * \phi} \quad (1)$$

Where ϵ_{510} is the molar absorptivity of the tris-phenanthroline complex ($11\ 100\ \text{cm}^{-1}\text{M}^{-1}$) that is formed when Fe^{2+} reacts with phenanthroline, l is the pathlength and ϕ is the quantum yield of the photodegradation of ferrioxalate into Fe^{2+} at the wavelength of irradiation (this value is tabulated for various wavelengths⁵⁵).

To estimate the quantum yield of S-to-O in solution, equation 2 was used⁵⁴, $d[O]/dt$ was determined by the initial absorption changes at 500 nm vs time, neglecting the absorption changes of the S-bonded isomer at this wavelength (this is reasonable since the molar absorptivity of the S-bonded isomer is ~ 4 times lower than for the O-bonded isomer at this wavelength, but this could result in a slight underestimation of the quantum yield). The molar absorptivity for the O-bonded isomer was estimated assuming full conversion into the O-bonded isomer following S-to-O photoisomerization. This is reasonable given the large differences in quantum yield for the forward and backward isomerization. The amount of light absorbed per volume (I_v) was determined using equation 3, where V is the volume of the sample and A_λ is the absorption at the wavelength of irradiation

$$\phi_{S \rightarrow O} = \frac{d[O]/dt}{I_v} \quad (2)$$

$$I_v = \left(\frac{I}{V}\right) * (1 - 10^{-A_\lambda}) \quad (3)$$

The quantum yield for the S-to-O photoisomerization on film was estimated in a similar way, but instead of using the amount of light absorbed per volume the amount of light per area was used. This value was determined by irradiating the ferrioxalate solution through a scaffold to obtain the area-normalized value, the films were then irradiated through the same scaffold. The amount of light absorbed per area (I_a) was determined with equation 4 where I is the photon flux, A_λ is the absorbance at the excitation wavelength and the area is the area of the scaffold.

$$I_a = \left(\frac{I}{\text{area}}\right) * (1 - 10^{-A_\lambda}) \quad (4)$$

The quantum yield was estimated with equation 6, monitoring the initial absorption changes at 500 nm. The surface coverage, Γ (moles per cm^2), was obtained using equation 5 where A_λ is the absorbance at the monitored wavelength and ϵ_λ is the molar absorptivity at that wavelength (which is assumed to be the same as in solution).

$$\Gamma = \frac{A_\lambda}{1000 * \epsilon_\lambda} \quad (5)$$

$$\phi_{S \rightarrow O} = \frac{d(\Gamma)/dt}{I_a} \quad (6)$$

O-to-S quantum yield of photoisomerization

The quantum yield for the O-to-S photoisomerization was estimated using Aberchrome 670 as the reference, similar to previously described⁵⁵ since the ferrioxalate reference is not suitable at wavelengths above 450 nm. Aberchrome 670 has a well-known quantum yield of photoisomerization that varies depending on the temperature and wavelength according to⁵⁵

$$\phi = 0.4326 - (3.285 * \lambda - 16.4 * T) * 10^{-4} \quad (7)$$

The photon flux (I) was determined by equation 8 (with ϕ known) using the supplementary software provided by Stranius et. al.⁵

$$\frac{d[A]}{dt} = - \frac{\phi * I * (1 - 10^{-Abs(t)})}{N_A * V} \quad (8)$$

With the photon flux known, the quantum yield for the O-to-S photoisomerization was determined with the same equation and software, instead using ϕ as the fitting parameter. This was done on fully isomerized samples with 590 nm irradiation to selectively excite the O-bonded isomer.

To estimate the photoisomerization quantum yield attached to the films, the same software was used but with equation 9 instead⁵⁵. Here, the sample and reference were irradiated through a mask to determine the area normalized photon flux.

$$\frac{dAbs}{dt} = - \frac{\phi * \epsilon_0 * 1000 * I * (1 - 10^{-Abs(t)})}{N_A * area} \quad (9)$$

References

1. Eskelinen, E.; Haukka, M.; Venäläinen, T.; Pakkanen, T. A.; Wasberg, M.; Chardon-Noblat, S.; Deronzier, A., Light-Induced Decarbonylation, Solvolysis, and Isomerization of Ru(L)(CO)₂Cl₂ (L = 2,2'-Bipyridine and 4,4'-Dimethyl-2,2'-bipyridine) in Acetonitrile. *Organometallics* **2000**, *19* (2), 163-169.
2. Rack, J. J., Electron transfer triggered sulfoxide isomerization in ruthenium and osmium complexes. *Coord. Chem. Rev.* **2009**, *253* (1-2), 78-85.
3. Hatchard, C. G.; Parker, C. A.; Bowen, E. J., A new sensitive chemical actinometer - II. Potassium ferrioxalate as a standard chemical actinometer. *Proceedings of the Royal Society of London. Series A. Mathematical and Physical Sciences* **1956**, *235* (1203), 518-536.
4. McClure, B. A.; Rack, J. J., Two-Color Reversible Switching in a Photochromic Ruthenium Sulfoxide Complex. *Angew. Chem. Int. Ed.* **2009**, *48* (45), 8556-8558.
5. Stranius, K.; Börjesson, K., Determining the Photoisomerization Quantum Yield of Photoswitchable Molecules in Solution and in the Solid State. *Sci. Rep.* **2017**, *7* (1), 41145.